High-Throughput Mechanomic Screening Reveals Novel Regulators of Single-Cell Mechanics

Laura Strampe[1], Katarzyna Plak[2,3], Christine Schweitzer[1], Cornelia Liebers[1,2], Paul Müller[1], Buzz Baum[3], Jona Kayser[1,*], and Jochen Guck[1,2,*]

[1]Max-Planck-Zentrum für Physik und Medizin & Max-Planck-Institute for the Science of Light, Erlangen, Germany
[2]Biotechnology Center, Center for Molecular and Cellular Bioengineering, Technische Universität Dresden, Dresden, Germany
[3]Medical Research Council Laboratory of Molecular Biology, Cambridge, United Kingdom
[*]Correspondence: jona.kayser@mpzpm.mpg.de, jochen.guck@mpzpm.mpg.de

ABSTRACT

The mechanical properties of cells are dynamic, allowing them to adjust to different needs in different biological contexts. In recent years, advanced biophysical techniques have enabled the rapid, high-throughput assessment of single-cell mechanics, providing new insights into the regulation of the mechanical cell phenotype. However, the molecular mechanisms by which cells maintain and regulate their mechanical properties remain poorly understood. Here, we present a genome-scale RNA interference (RNAi) screen investigating the roles of kinase and phosphatase genes in regulating single-cell mechanics using Real-Time Fluorescence and Deformability Cytometry (RT-FDC). Our screen identified 82 known and novel mechanical regulators across diverse cellular functions from 214 targeted genes, leveraging RT-FDC's unique capabilities for comprehensive, high-throughput mechanical phenotyping with single-cell and cell cycle resolution. These findings refine our understanding of how signaling pathways coordinate structural determinants of cell mechanical phenotypes and provide a starting point for uncovering new molecular targets involved in biomechanical regulation across diverse biological systems.

SIGNIFICANCE

Cell mechanical properties are tightly regulated and play pivotal roles in processes ranging from tissue morphogenesis to disease progression. Despite their importance, the genetic regulation of single-cell mechanics remains largely unexplored. This study represents one of only a few large-scale mechanomic investigations conducted to date. It is the first study to leverage RT-FDC's unique capability for high-throughput mechanical phenotyping with single-cell and cell cycle resolution to detect gene impacts that may be overlooked in lower-throughput or population-level studies. The mechanical genes identified here provide valuable data points for understanding how cells control their mechanical state and serve as a foundation for future studies exploring the molecular basis of biomechanical regulation.

INTRODUCTION

Cell mechanics encompasses all physical interactions between a cell and its surroundings, including how cells generate, sense, and respond to mechanical forces. These mechanical properties are fundamental to numerous physiological processes, such as migration, proliferation, and differentiation (1–3), and are increasingly recognized as critical factors in pathological conditions, including cancer progression and immune responses. One key aspect of cell mechanics is cell stiffness, which describes how much a single cell deforms under external forces. Stiffer cells resist deformation, while softer cells deform more readily. Variations in cell stiffness have been implicated as biomarkers of diverse physiological and pathological states. For instance, during chemically induced osteoblast differentiation of mesenchymal stem cells, cell softening outperformed traditional molecular biomarkers as a reliable indicator of differentiation (4). Red blood cells stiffen in pathological conditions such as sickle cell anemia, spherocytosis, malaria, and COVID-19 infection (5–8). In malaria, increased red blood cell stiffness elevates the risk of microcapillary obstruction and correlates with fatal patient outcomes (9). A more dynamic response is observed in neutrophils during immune response: they initially stiffen upon activation but soften significantly within 15 minutes, potentially aiding their migration towards the inflammation site (10). Similarly, single metastatic cancer cells are consistently

softer than their healthy counterparts (11–13), in contrast to tumors, which tend to be stiffer than the surrounding healthy tissue as a whole (14). This softening in metastatic cancer cells is hypothesized to improve their ability to navigate dense tissue environments, enabling invasive behaviors such as tissue infiltration and intra- and extravasation (15). Another possibility is immune evasion, as softer cancer cells are not as readily killed by cytotoxic T-cells (16).

Despite extensive evidence correlating cell stiffness with disease states, the genetic and functional determinants of mechanical phenotypes remain poorly understood. Addressing this knowledge gap is the primary goal of mechanomics, a relatively new subfield of cell mechanics that attempts to connect the mechanical phenotype of cells to a comprehensive understanding of the underlying genotype. Current knowledge identifies the contractile actomyosin cortex as the primary regulator of cell stiffness. This dynamic network of actin filaments generates contractile forces through myosin motor proteins, with its activity tightly controlled by Rho signaling (17). Additional structural determinants of cell mechanics include other cytoskeletal proteins such as microtubules, intermediate filaments and septins, the lipid plasma membrane, the nucleus, and macromolecular packing in the cytoplasm (15). While cytoskeletal drugs can modulate cell stiffness by disrupting the different cytoskeletal filaments, they often induce cytotoxic effects (18, 19), limiting their utility in functional studies. Genetic approaches such as RNA interference (RNAi) could provide a more precise and less invasive means of modulating cell mechanics. RNAi achieves gene knockdown by introducing short RNA strands that bind to corresponding mRNA transcripts, preventing their translation into proteins (20). Large-scale RNAi screens systematically evaluate the effects of individual gene knockdowns, enabling the precise identification of key genetic regulators of cell stiffness. Previous mechanomic RNAi screens using atomic force microscopy (AFM) identified both known and novel regulators of actin organization and cortical stiffness (21, 22). However, the low throughput of AFM limited the number of cells analyzed per gene, raising concerns about statistical power and reproducibility. Alternatively, transcriptomics-based mechanomics has been used to correlate gene expression with mechanical phenotypes, offering insights into the collective effects of many genes, though it lacks the precision of targeted knockdown approaches (23). The common fruit fly *Drosophila melanogaster* serves as an ideal model organism for RNAi studies due to its relatively simple genome, conservation of many human homologs, and the efficiency of RNA strand uptake (24, 25).

Real-Time Fluorescence and Deformability Cytometry (RT-FDC) has emerged as a powerful high-throughput technique for characterizing cell mechanics at the single-cell level (26). Cells are suspended in a viscous measurement buffer and subjected to hydrodynamic shear forces as they flow through a narrow microfluidic channel. Through high-speed image analysis, RT-FDC measures how much each cell deforms, from which its apparent Young's modulus can be estimated (27). This method is capable of analyzing up to 100 cells per second, enabling the rapid mechanical profiling of entire cell populations while retaining single-cell resolution (28). In addition, RT-FDC enables subcellular localization of fluorescent proteins, enabling the differentiation of interphase and mitotic cells by detecting nuclear envelope breakdown (29). This allows for the separate mechanical phenotyping of both cell cycle phases in phase-mixed cell populations.

RT-FDC's potential for mechanomic screening was first demonstrated by Rosendahl et al. (29) through a targeted RNAi screen of 42 genes associated with actin cortex regulation. This study confirmed the critical role of Rho signaling in controlling cell stiffness but remained limited to a small gene set previously known to influence the actin cytoskeleton. RT-FDC was subsequently applied in a clinical context for biophysical phenotyping of circulating immune cells in systemic sclerosis patients (30). In this work, we significantly expand the scope of RT-FDC-based mechanomic screening by targeting 214 kinase and phosphatase genes in *Drosophila melanogaster*. Kinases and phosphatases modulate protein activity through reversible phosphorylation, inducing conformational changes that switch proteins between active and inactive states (31). These enzymes regulate numerous downstream signaling pathways, making them ideal candidates for identifying novel genetic regulators of cell mechanics. Our study not only identifies potential new regulators of cell stiffness but also emphasizes the distinct advantages of incorporating cell cycle resolution into mechanomic screening. We demonstrate that resolving mechanical phenotypes at the single-cell and cell cycle level uncovers phase-specific gene functions, prevents the identification of apparent stiffening effects caused by shifts in cell cycle distribution, and improves the accuracy and reliability of mechanical hit detection.

MATERIALS AND METHODS

Cell culture

The semi-adherent *KC167* cell line (*Drosophila melanogaster*), stably expressing nuclear NLS-GFP and cytoplasmic tdTomato (29), was cultured in Shield and Sang M3 Insect Medium (Sigma Aldrich, Darmstadt, Germany, S3652) supplemented with 10 % Fetal Bovine Serum (FBS, Sigma Aldrich, Darmstadt, Germany, F7524) and 1 % Penicillin-Streptomycin (Pen-Strep, Thermo Fisher, Darmstadt, Germany, 15070063). The FBS was heat-inactivated for 30 minutes at 56 °C. This complete growth medium was stored at room temperature for up to two weeks. The cells were cultured in T25 cell culture flasks (Greiner Bio-One, Frickenhausen, Germany, 690175) at 24 °C without CO_2. Growth medium was exchanged every other day. Cells were passaged once a week. For passaging, the old culture medium was removed and the cells were resuspended in 2 ml of fresh

complete growth medium by repetitive pipetting. 300 µl of this cell suspension was then added to a new T25 flask containing 4 ml of complete growth medium.

Gene knockdown via RNA interference

RNA interference (RNAi) was induced in the *KC167* cells via transfection with double-stranded RNA (dsRNA). We used a subset of the Heidelberg 2 dsRNA library (HD2 or BKN library) (32), targeting 143 phosphatase genes and 71 genes (see Table S1). The library contains two different dsRNA strand for each target gene. Sequence information for all strands can be accessed via the RNAi identifier under http://www.genomernai.org/.

Cells were harvested for dsRNA transfection at 60% to 80% confluency. They were removed from the culture flask and resuspended in fresh medium (see passaging protocol described above) and then centrifuged at 100 ×g and room temperature for 5 minutes to form a cell pellet. The cells were then washed with 3 ml of Dulbecco's phosphate-buffered saline (DPBS, Thermo Fisher, Darmstadt, Germany, 14190250), which has been adjusted to a pH of 6.8 and an osmolality of 320 mOsm/kg and is hereafter referred to as Drosophila-PBS. pH was adjusted through addition of NaOH or HCl, osmolality was adjusted through addition of NaCl. After washing, the cells were centrifuged again as described above and resuspended in 500 µl serum-free medium (Shield and Sang M3 Insect Medium supplemented with 1 % Pen-Strep). The cells were then counted using the Countess II Automated Cell Counter (Thermo Fisher, Darmstadt, Germany, AMQAX1000) by diluting 10 µl of the cell suspension in 40 µl of Drosophila-PBS and staining the diluted cells 1:1 with Trypan Blue (Thermo Fisher, Darmstadt, Germany, T10282). Based on this cell count, the cell suspension was further diluted with serum-free medium to reach a final concentration of $5x10^6$ cells/ml.

For each knockdown sample, 2.7 µl of dsRNA from the BKN library (1 µg/µl stock solution) was mixed with 45 µl serum-free cell suspension. For the control samples, 2.7 µl of Tris-EDTA buffer (Sigma Aldrich, Darmstadt, Germany, 93283) was used instead. The cell-dsRNA mix was transferred to a 24-well plate (Greiner Bio-One, Frickenhausen, Germany, 662160), where it was placed as a single droplet in the center of the well and left to settle for 1 hour. The well was then filled with 400 µl of complete growth medium and incubated for 4 days at 24 °C without CO_2. After 2 days of incubation, 300 µl of additional complete growth medium was added to the well and the cells were resuspended by repetitive pipetting.

Enrichment of the mitotic fraction

Given the typically small number of mitotic cells in asynchronous cell populations, we enriched the mitotic fraction of each cell sample through incubation with 50 µM Colchicine (Thermo Fisher, Darmstadt, Germany, J61072.06) prior to the mechanical phenotyping measurement. For this, the Colchicine stock solution (100 mM in ethanol) was diluted at a 1:2000 ratio in complete growth medium. After removal of the dsRNA-medium from the knockdown sample well, 300 µl of diluted Colchicine was added to the well and incubated in the dark for 5 hours. This treatment has been shown to increase the fraction of mitotic cells in *KC167* cultures from approximately 5 % to up to 17 % (29).

Mechanical phenotyping using Real-Time Fluorescence and Deformability Cytometry (RT-FDC)

Mechanical measurements took place 4 days after RNAi knockdown treatment. The RT-FDC setup, measurement procedures and real-time image analysis protocols have been described in detail in (29). For this study, we used microfluidic chips with a microfluidic channel width of 20 µm and a total flow rate of 0.04 µl/s. Fluorescence traces were collected in the green 525/50 nm channel for nuclear NLS-GFP, and in the red 593/46 nm channel for cytoplasmic tdTomato. The viscous measurement buffer used for this study was prepared by supplementing Drosophila-PBS (described above) with 0.5% (w/v) methylcellulose (Fisher Scientific, Reinach, Switzerland, 11374247), hereafter referred to as MC. The MC was warmed to room temperature and sterile filtered through a 0.22 µm PVDF filter (Merck, Darmstadt, Germany, SLGV033RB) before measurements. Cell were collected and centrifuged into a cell pellet as described above, and then resuspened in MC and loaded onto the microfluidic chip for mechanical phenotyping as described by Rosendahl et al. (29). In total, at least 2000 single cells were measured for each cell sample.

All measured RT-FDC datasets are available on the Deformability Cytometry Open Repository (DCOR) under https://dcor.mpl.mpg.de/organization/mechano-genomic-screening. DCOR is an effort towards making Deformability Cytometry (DC) data easily accessible to anyone. DCOR serves DC datasets (normally around 25 GB in size) for download or for online data analysis using the graphical user interface Shape-Out (https://shapeout.readthedocs.io). In addition, DCOR facilitates sharing and organizing DC data online. The public DCOR instance at https://dcor.mpl.mpg.de is free to use for the general public. For private projects, it is also possible to self-host DCOR. More information can be found at

https://dc.readthedocs.io.

Post-experimental data analysis was performed using the python package dclab version 0.62.6 (available at https://github.com/DC-analysis/dclab). Measured cells were filtered based on the following parameters (explained in detail in (33)): cross-sectional cell area between 20 and 200 μm^2, porosity (also called area ratio) between 1 and 1.05 and maximum fluorescence intensities in both channels between 400 and 40000 intensity units. In addition, manual gating of cell position within the bright-field image versus peak position of the fluorescence trace was used to ensure proper matching between the two. Manual gating was also used to separate the interphase and mitotic subpopulations within each sample based on peak widths in the two fluorescence channels (compare Fig. 2A). Young's modulus values were calculated based on a cell's area and deformation using the lookup table LE-2D-FEM-19 implemented in dclab.

Screening procedures and statistical analysis

For each target gene, at least 5 biological replicates using two different dsRNA strands were measured. Genes are divided into three groups (*kin* for all kinases and *phos1*/*phos2* for phosphatases) which were consecutively measured. For experimental blinding, all dsRNA strands, even those targeting the same gene, were assigned unique sample IDs within their group (see Table S1). Replicates of the same sample ID were measured on different days, with a few weeks distance between consecutive measurements. On each measurement day, around 10 different gene knockdowns and at least independent 2 control samples were measure, with the first measurement of the day always being a control. The same microfluidic chip was used for all measurements of a day, except for when clogging in the microfluidic channel necessitated an exchange of the chip. In that case, an additional control sample was measured directly after chip exchange. Between measurements, 50 µl of MC was loaded onto the chip to separate samples. During analysis, each knockdown measurement was matched to the temporally closest control measurement that used the same chip.

Statistical analysis was performed using a linear mixed model to estimate mean differences in Young's modulus distributions between knockdown samples and matched daily controls (34). This model accounts for baseline variability in Young's modulus values across experimental days, caused by changes in environmental conditions or knockdown efficiency. Significance was determined using a likelihood ratio test, which is robust against the large sample sizes typical of RT-FDC datasets. A gene was identified as a mechanical hit, if mean Young's modulus between knockdown samples and controls differed with $p < 0.05$. For the mitotic downsampling reanalysis, mean differences and p-values were averaged over 10 downsampling repetitions to account for stochastic variability. Graphs were generated using the python packages matplotlib and seaborn. Schematics were created in BioRender and Adobe Illustrator. BioRender schematics can be accessed via https://BioRender.com/f63v496.

RESULTS

Population-wide single-cell mechanics screening using RT-FDC

The mechanical phenotype of single cells plays a fundamental role in both physiological and pathological processes, yet how cells regulate and maintain their mechanical state remains poorly understood. To systematically investigate how genetic perturbations influence single-cell mechanics, we performed a genome-scale RNA interference (RNAi) knockdown screen (Fig. 1A) targeting 143 phosphatase genes and 71 additional kinase genes in the *Drosophila* genome using the Heidelberg 2 (BKN) RNAi library (32). Kinase and phosphatase genes were selected as unbiased targets due to their central roles in cellular signaling, without prior selection based on known interactions with cell mechanics. This exploratory approach aimed to uncover novel links between signaling pathways and mechanical phenotype regulation.

To quantify changes in cell mechanics upon gene knockdown, we used Real-Time Fluorescence and Deformability Cytometry (RT-FDC), a high-throughput microfluidic mechanical phenotyping technique (Fig. 1A). While RT-FDC has previously been applied in a broad range of smaller scale studies (29, 30, 35, 36), it has never before been used for large-scale mechanomic screening. RT-FDC measures cell stiffness by subjecting cells to hydrodynamic shear forces as they flow through a narrow microfluidic channel. Real-time bright-field imaging captures cell deformation, from which an apparent Young's modulus value is derived to quantify cell stiffness. Softer cells, with lower Young's modulus values, assume a bullet-like shape, while stiffer cells retain a more circular profile.

A key advantage of RT-FDC for screening applications is its ability to measure up to 100 cells per second, enabling the collection of thousands of single-cell stiffness measurements per gene knockdown (Fig. 1B). This comprehensive sampling captures the full mechanical heterogeneity within a cell population, which is critical given that across all measurements performed for this screen, the standard deviation of Young's modulus within one sample typically was around 0.24 kPa, while mechanical knockdown effects were around 0.04 kPa in magnitude. Such biological variability underscores the need for population-wide single-cell measurements to reliably detect smaller mechanical knockdown effects and to minimize sampling bias which can affect lower-throughput techniques such as atomic force microscopy (AFM), which only supports measurements

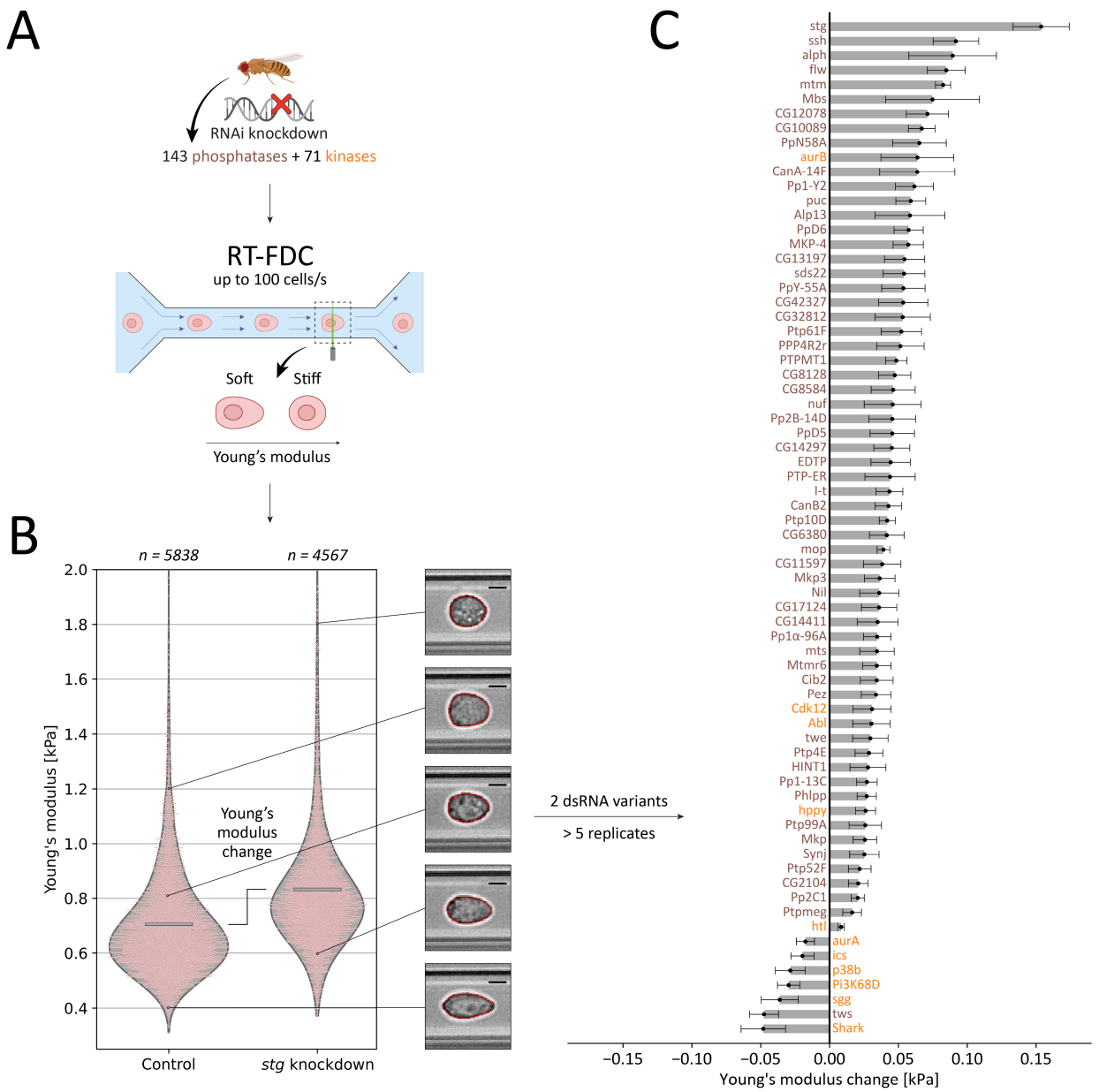

Figure 1: Mechanical knockdown screen of 214 kinase and phosphatase genes. **A** Overview of the mechanomic screening workflow. For each target gene, RNAi knockdown was performed in the *Drosophila* cell line *KC167*. Real-Time Fluorescence and Deformability Cytometry (RT-FDC) was used to measure the stiffness of at least 2000 single cells for each knockdown sample via hydrodynamic deformation in a microfluidic channel. Cell stiffness was quantified as Young's modulus, with stiffer cells having higher Young's modulus values. **B** Typical Young's modulus distributions, measured in *stg* knockdown cells and their matched daily control sample. Each pink dot represent a single cell measurement. Five representative single cell measurements at different stiffness values are annotated with their corresponding bright-field microscopy images. Scale bars are 5 µm. For the control sample, 9 measurements are above the plot window going up to 5.6 kPa. For the knockdown sample, 35 measurements are above the plot window going up to 6.5 kPa. **C** Knockdown effect of all mechanical hits (70/214). For each target gene, at least five biological replicates were measured using two distinct dsRNA strands. Genes causing a significant ($p < 0.05$) change in mean Young's modulus are regarded as mechanical hits. Positive Young's modulus changes indicate cell stiffening, negative changes indicate cell softening upon gene knockdown. Phosphatase genes are labeled in brown, kinase genes in orange. Mean difference calculation, error margin estimation and significance testing were performed through linear mixed model analysis.

of a few cells per condition in larger screens (22).

Among the 214 targeted genes, we identified 70 mechanical hits that significantly shifted the mean Young's modulus of the knockdown cell samples compared to matched daily controls (Fig. 1C). The vast majority of these mechanical hits caused cell stiffening upon knockdown (63 genes). These cell stiffening genes are mostly phosphatases. In contrast, only seven knockdowns led to cell softening, six of which were caused by kinase genes. The strongest mechanical effect observed upon knockdown of the mitotic regulator String (*stg*), which resulted in a 0.15 kPa increase in stiffness.

Cell cycle-resolved analysis reveals additional softening effects

Of the 70 mechanical hits identified in our screen, 63 increased mean Young's modulus, while only seven caused cell softening. Additionally, phosphatase and kinase genes were well separated by their knockdown effects: phosphatase knockdowns predominantly led to cell stiffening, while kinase knockdowns resulted in cell softening. This suggests that phosphatase function generally maintains cell softness, whereas kinases maintain cell stiffness. However, the 9:1 ratio of stiffening to softening hits far exceeds the twofold difference in the number of targeted phosphatases versus kinases. This discrepancy indicates that factors beyond the higher number of phosphatases in our target set may contribute to the large number of cell stiffening phenotypes observed in our screen.

One possible explanation is that gene knockdowns affect cell mechanics not only by altering single-cell mechanical properties but also by influencing population-level characteristics, such as cell cycle fractions. As cells progress through the cell cycle, their mechanical properties change, with mitotic cells being significantly stiffer than interphase cells (37). Therefore, gene knockdowns that increase the fraction of mitotic cells in a sample could lead to an apparent stiffening of the whole cell population, even without direct effects on single-cell mechanical properties. To investigate this possibility, we leveraged the cell cycle resolution capabilities of RT-FDC, initially introduced by Rosendahl et al. (29), to separately analyze mechanical changes in the interphase and mitotic subpopulations of each gene knockdown sample.

RT-FDC achieves simultaneous mechanical phenotyping and cell cycle classification through fluorescence-based protein localization combined with bright-field imaging (Fig. 2A). As a cell flows through the microfluidic channel (compare Fig. 1A), fluorescence intensity curves reveal the intracellular distribution of labeled nuclear and cytoplasmic proteins. Interphase cells, with intact nuclei, exhibit a sharp nuclear fluorescence peak distinct from the broader cytoplasmic peak. Mitotic cells, characterized by nuclear envelope breakdown, show fluorescence peaks of equal width due to the release of the nuclear content into the cytoplasm. These distinct signatures enable real-time cell cycle classification, allowing independent comparisons of the Young's modulus distributions in the interphase and mitotic subpopulations.

To assess how changes in cell cycle fractions influence apparent mechanical phenotypes, we performed a cell cycle-resolved analysis of our screen data by separately comparing mean Young's modulus values between knockdown and control conditions within the interphase and mitotic subpopulations of each gene knockdown sample (Fig. 2B and Fig. 3A). Of the 70 genes originally identified as mechanical hits in the full population analysis, 58 remained significant in at least one cell cycle phase (purple section in Fig. 3A). Among these, 11 genes influenced both interphase and mitotic cells, 42 genes affected only interphase cells and just five genes exclusively changed the mechanical phenotype of mitotic cells. Of all 16 full population hits that influence mitotic mechanics, only one gene knockdown caused cell softening (*tws*), while all other caused cell stiffening.

Beyond confirming mechanical hits identified in the full population analysis, cell cycle resolution uncovered 22 additional hits (pink section in Fig. 3A). In contrast to the predominance of stiffening phenotypes identified in the full population analysis, the majority of these newly uncovered hits induced cell softening. 10 genes exclusively softened mitotic cells, a phenomenon entirely absent from the full population results. There, the only mitotic softening gene was *tws*, which also softened interphase cells. Together with the five newly identified interphase-softening genes, the cell cycle-resolved analysis more than doubled the number of cell softening phenotypes identified in our screen. Notably, the newly identified softening hits were predominantly phosphatases, challenging the earlier association between kinase knockdown and cell softening. This suggests that the prior correlation between both may have been a statistical artifact resulting from the limited total number of softening hits, rather than reflecting a true biological distinction between kinase and phosphatase function.

Among the newly identified genes, *PRL-1* and *aurA* stand out by exhibiting opposing mechanical effects between the cell cycle phase. Knockdown of the phosphatase *PRL-1* stiffened interphase cells while softening mitotic cells, whereas knockdown of the kinase *aurA* softened interphase cells and stiffened mitotic cells. As the bidirectional knockdown effect of *PRL-1* directly counteracted the mechanical oscillations associated with cell cycle progression, it was uniquely revealed through cell cycle resolution.

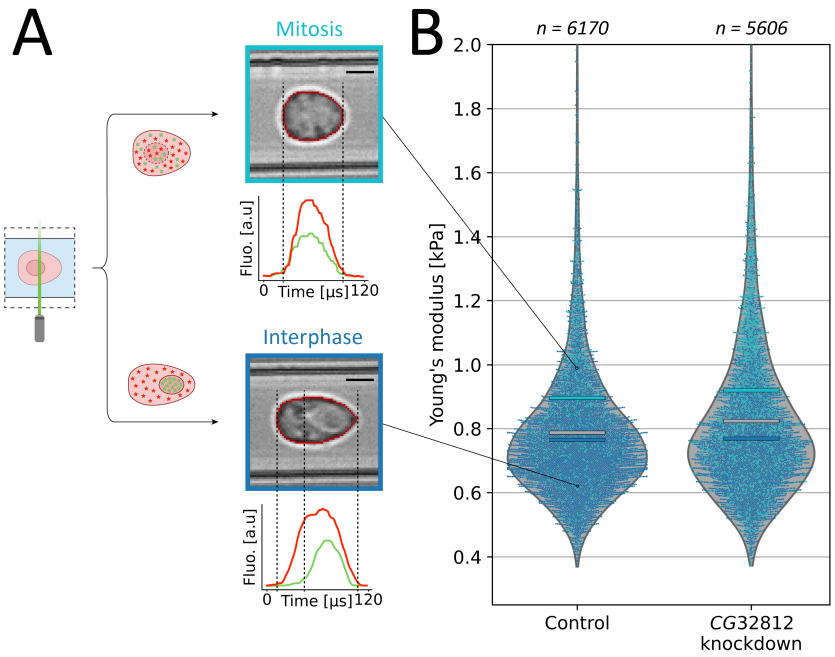

Figure 2: Cell cycle resolution in Real-Time Fluorescence and Deformability Cytometry (RT-FDC). **A** Classification of interphase and mitotic cells based on nuclear envelope breakdown. For each cell cycle phase, one representative single cell measurements from the control sample is annotated with its bright-field microscopy image and fluorescence traces (red for cytoplasmic tdTomato, green for nuclear NLS-GFP). Scale bars are 5 µm. **B** Young's modulus distributions with cell cycle classification, measured in *CG32812* knockdown cells and their matched daily control sample. Each dot represent a single cell measurement, with the blue dots representing cells in interphase and cyan dots representing cells in mitosis. Horizontal lines represent mean Young's modulus for the full cell population (gray), as well as for the interphase (blue) and mitotic (cyan) subpopulations. For the control sample, 15 measurements are above the plot window going up to 5.4 kPa. For the knockdown sample, 31 measurements are above the plot window going up to 5.6 kPa.

Mitotic fraction changes drive apparent stiffening in full population analysis

While most mechanical hits from the full population analysis remained significant in the cell cycle-resolved analysis, 12 full population hits did not cause any significant mechanical effect in either interphase or mitosis (red section in Fig. 3A). All these genes encode phosphatases and caused relatively small stiffening effects in the full population analysis (compare Fig. 1C). Since all these hits were associated with increased stiffness, we hypothesized that their full population effects may reflect knockdown-induced shifts in cell cycle distribution rather than genuine changes in single-cell stiffness. Since mitotic cells are inherently stiffer than interphase cells, an increase in the number of mitotic cells upon gene knockdown could artificially increase the mean Young's modulus in the full knockdown population. A illustrative example for this process is provided by the knockdown of *CG32812* (Fig. 2B), where an increased mitotic fraction in the knockdown sample shifts the mean stiffness of the full population upwards, while the Young's modulus means in the interphase and mitotic subpopulation remain almost unchanged.

To test whether increased mitotic fractions generally correlated with apparent stiffening effects, we compared changes in mitotic fraction across all identified mechanical hits (Fig. 3B). Genes identified as mechanical hits in both full population and cell cycle-resolved analyses typically showed a 4% increase in mitotic cells compared to controls. In contrast, hits exclusively identified through cell cycle-resolved analysis exhibited a significantly smaller increase in mitotic fraction of around 2%. Genes which only influenced mechanics in the full population showed the largest mitotic fraction increases of around 7%, with only one gene (*Abl*) exhibiting a decreased mitotic fraction upon knockdown. These findings support our hypothesis that knockdown-induced increases in mitotic cell numbers, rather than changes in individual cell stiffness, contributed to many of the apparent mechanical phenotypes in the full population analysis.

To directly test this hypothesis, we performed a mitotic downsampling reanalysis of our data (Fig. 3C). For each full population hit exhibiting increased mitotic fractions, we reduced the number of mitotic cells in the knockdown samples by

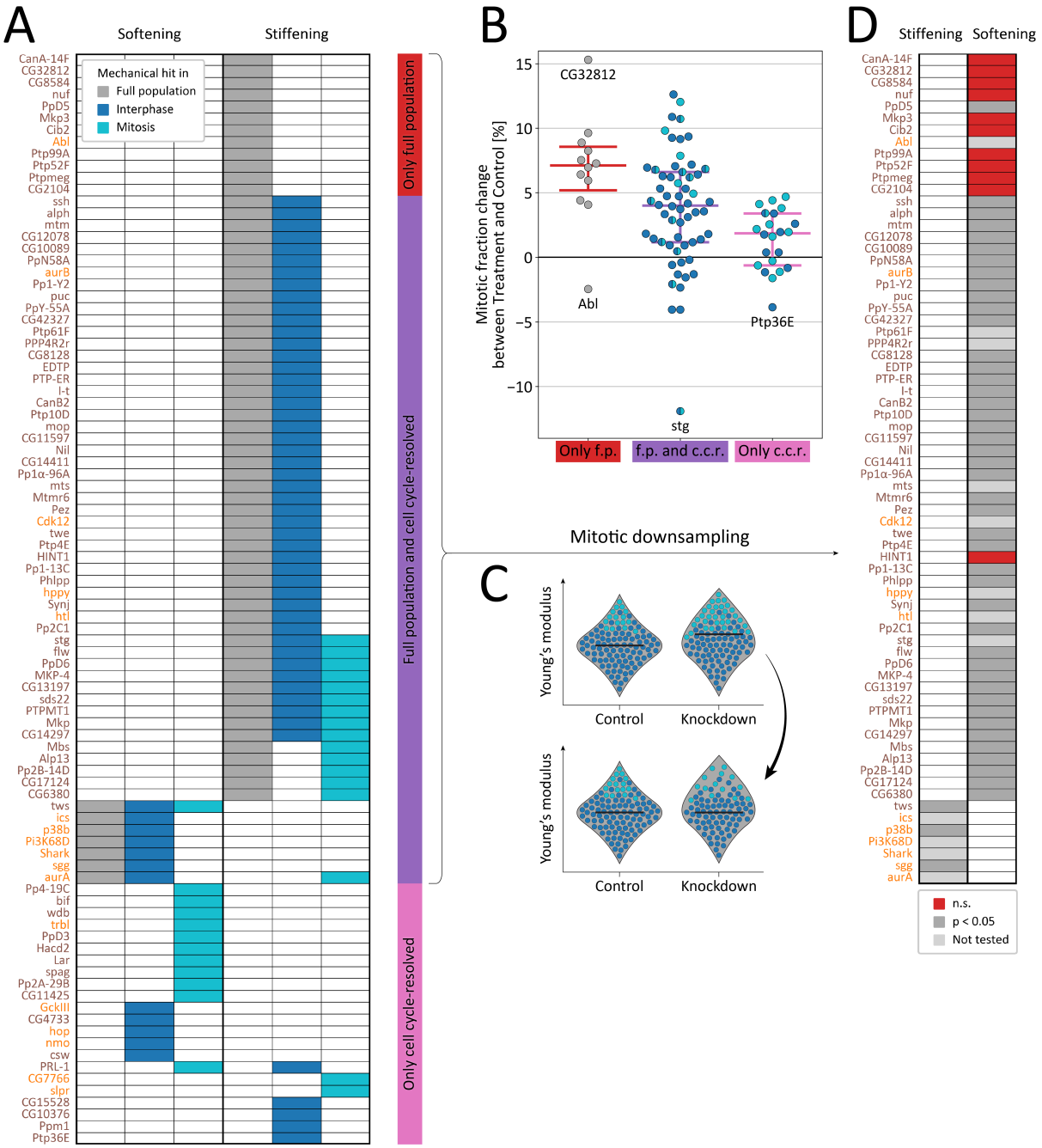

Figure 3: Cell cycle-resolved analysis of the mechanical knockdown screen of 214 kinase and phosphatase genes. **A** Comparison of mechanical hits identified from comparing mean Young's modulus values between the full cell populations (gray, see Fig. 1) and from separately comparing control and knockdown means in the interphase (blue) and mitotic (cyan) subpopulations. Hits are separated into softening (Young's modulus change < 0) and stiffening (Young's modulus change > 0). Phosphatase genes are labeled in brown, kinase genes in orange. **B** Difference in mitotic fraction $n_{\text{mitotic}}/n_{\text{total}}$ between gene knockdown and control samples for all mechanical hits reported in A, categorized by the analysis method that identified them as the hits, f.p. for full population, c.c.r. for cell cycle-resolved. Marker colors indicate the (sub)-populations in which the significant changes in Young's modulus were observed. Horizontal lines represent mean and mean standard deviation. Outliers are labeled with their gene symbol. **C** Schematic illustration of mitotic downsampling workflow. **D** Significance of the mechanical gene knockdown effect after mitotic downsampling. Genes with a mitotic fraction change < 0 were not tested. Significance testing for A and D was performed through linear mixed model analysis.

randomly removing mitotic cells until the mitotic fraction matched that of the corresponding control. We then repeated the full population analysis to determine whether the previously observed mechanical phenotypes persisted even without the influence of increased mitotic fractions (Fig. 3D). After correcting for mitotic fraction shifts via mitotic downsampling, 10 out of the 12 genes exclusively identified in the full population analysis no longer showed significant stiffening effects. All other mechanical hits, except *HINT1*, retained their significance. These results demonstrate that most stiffening effects observed exclusively in the full population analysis can be attributed to shifts in cell cycle distribution instead of genuine changes in single-cell mechanics. The fact that *Abl* and *PpD5* knockdowns caused significant cell stiffening in the full population analysis, even without any mitotic fraction increase, despite showing no significant effects in either interphase or mitotic subpopulations individually, suggests the presence of a more complex knockdown response that cannot be fully captured by analyzing interphase and mitotic populations separately. In contrast, the loss of significance for *HINT1* following mitotic downsampling indicates that its comparatively weak stiffening phenotype (compare Fig. 1C) was only significant in the full population due to an accompanying increase in mitotic fraction.

Taken together, our results demonstrate how cell cycle resolution can improve mechanomic screening. By separately analyzing mechanical phenotypes in the interphase and mitotic subpopulations, we both identified previously undetectable mitosis-specific and softening knockdown effects and eliminated apparent mechanical hits, which falsely attribute full population mechanical changes to genuine single-cell effects rather than shifts in cell cycle distribution.

Known and novel regulators in diverse cellular functions

After identifying additional hits and eliminating apparent stiffening effects through cell cycle resolution, we obtained a final set of 82 mechanical hits among the 214 tested kinase and phosphatase genes. To evaluate the impact of our screen, we classified these genes into three categories based on literature: known mechanical regulators, mitotic regulators, and novel candidate genes without prior links to cell mechanics or mitosis (Fig. 4).

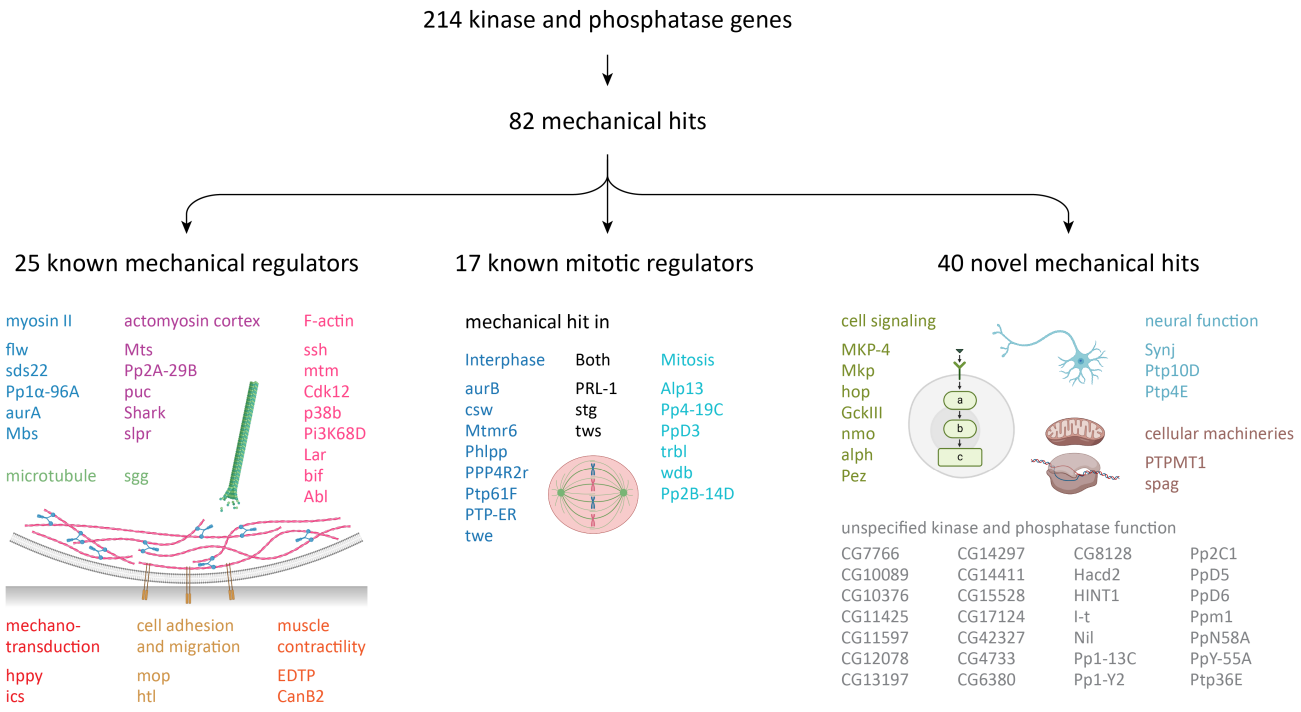

Figure 4: Classification by gene function of the 82 mechanical hits identified in our mechanomic screen according to literature. Mechanical regulators only implicated in regulation of mitotic mechanics are classified together with regulators of cell cycle progression through mitosis as mitotic regulators. Genes neither known for mechanical nor mitotic regulation are classified as novel mechanical hits. For known mechanical regulators and novel genes, colors indicate subclasses of cell function. For all subclasses except actomyosin cortex, mechanotransduction, muscle contraction and unspecified kinase and phosphatase function, text colors correspond to component colors used in the schematic drawings. For known mitotic hits, colors indicate the cell cycle in which the mechanical effects identified in this screen were identified. Literature sources in Tables 1,2 and 3.

25 genes were classified as known mechanical regulators, validating RT-FDC as a robust screening platform. Most of these genes are involved in actomyosin regulation, either through regulation of cortical tension via JNK signaling (*puc*, *Shark*, *slpr*) or as components of the PP2A complex (*Pp2A-29B*, *mts*). Others contribute to F-actin filamentation and organization (*ssh*, *mtm*, *Cdk12*, *p38b*, *Pi3K68D*, *Lar*, *bif*, *Abl*) or the phosphorylation of the non-muscle myosin II regulatory light chain (*Mbs*, *flw*, *PP1β9c*, *sds22*, *AurA*). Beyond actomyosin regulation, the screen identified genes linked to diverse mechanical cell functions. Some play roles in F-actin organization during adhesion and migration (*mop*, *htl*), while others contribute to mechanotransduction (*hppy*, *ics*) or indirect flight muscle (IFM) contractility in *Drosophila* (*EDTP*, *CanB2*). Regulation of the microtubule cytoskeleton was also represented (*sgg*). The identification of genes spanning multiple known mechanics-related pathways highlights the versatility of RT-FDC-based mechanical phenotyping, demonstrating its potential for systematically mapping genetic regulators of cell mechanics.

Several mechanical hits were previously associated with microtubule dynamics during mitotic spindle assembly, including *wrd*, *aurB*, and *Pp4-19C* (38, 39). These genes were not included in the known mechanical regulators category but were instead grouped as mitotic regulators. Since mitosis inherently involves mechanical processes such as cytoskeletal reorganization and spindle assembly, most mitotic regulators were expected to affect cell stiffness, either directly or indirectly, particularly in mitotic cells. In total, we identified 17 known mitotic regulators whose knockdown significantly altered cell mechanics. Of these, nine genes changed mechanics of mitotic cells (*stg*, *Alp13*, *Pp2B-14D PpD3*, *trbl*, *PRL-1*, *Pp4-19C*, *tws*, *wdb*). Notably, three of theses mechanical hits in mitosis (*stg*, *PRL-1*, *tws*) and eight additional genes (*aurB*, *Ptp61F*, *PPP4R2r*, *PTP-ER*, *Mtmr6*, *twe*, *Phlpp*, *csw*) also cause a significant mechanical shift in the interphase cell population. This indicates that these genes have regulatory roles beyond mitosis, suggesting previously unrecognized gene functions in interphase cell mechanics.

Finally, our screen identified 40 genes with no prior connection to either cell mechanics or mitosis. This set includes well-characterized genes involved in various signaling pathways (*MKP-4*, *Mkp*, *hop*, *GckIII*, *nmo*, *alph*, *Pez*), as well as genes linked to neural function (*Synj*, *Ptp10D*, *Ptp4E*) and genes involved in assembly and activity regulation of cellular machineries (*spag*, *PTPMT1*). All other mechanical hits in this category have not been characterized beyond their general kinase and phosphatase function. The identification of such diverse novel mechanical regulators underscores the power of RT-FDC for genome-scale mechanical screening in uncovering novel regulatory pathways and provides a foundation for future studies exploring the genetic basis of single-cell mechanics.

DISCUSSION

Cells actively regulate their mechanical properties to adapt to changing biological contexts, yet the mechanistic links between genotype and single-cell mechanical phenotype remains poorly understood. In this study, we presented a genome-scale RNA interference (RNAi) knockdown screen of kinase and phosphatase impact on single-cell mechanics using Real-Time Fluorescence and Deformability Cytometry (RT-FDC).

Cell cycle resolution improves mechanical screening

Our screen utilized the cell cycle resolution capabilities of RT-FDC to separately analyze the mechanical effect of gene knockdown on interphase and mitotic cells. We demonstrated that compared to the full population analysis, the cell cycle-resolved analysis identified additional mechanical hits, decreased bias by uncovering softening and mitosis-specific effects overlooked by full population analyses, and effectively eliminated apparent stiffening effects that were caused by knockdown-induced shifts in cell cycle distribution rather than genuine changes in single-cell mechanics.

One mechanical hits uniquely identified by the cell cycle-resolved analysis was *PRL-1*, which directly counteracted the mechanical oscillations associated with cell cycle progression by stiffening interphase cells and softening mitotic cells. This bidirectional mechanical shift upon *PRL-1* knockdown suggests that overexpression of *PRL-1* may amplify these mechanical oscillations, broadening the range of mechanical phenotypes a single cell can adopt. Given *PRL-1*'s established role as a cancer metastasis marker (40), such mechanical adaptability could facilitate tumor progression by enhancing a cell's ability to overcome physical constraints, including detachment from the primary tumor, migration through dense tissues, and invasion into and out of the vasculature. This hypothesis aligns with findings from epithelial–mesenchymal transition (EMT), a key process in cancer metastasis, where breast epithelial cells were shown to stiffen in mitosis and soften in interphase, increasing single-cell mechanical variability (41). The discovery of *PRL-1* therefore highlights the strength of cell cycle resolution in uncovering biologically relevant gene functions that remain obscured in population-wide analyses.

Comparison with previous mechanomic screens

The genome-scale mechanical screen presented in this work significantly expands the scope of deformability cytometry-based screens, surpassing prior studies which were limited to smaller target groups, such as 42 cytoskeletal regulator genes (29) or a

limited number of chemical compounds (42). In contrast, our study evaluated a comprehensive set of 143 phosphatase genes and an additional 71 kinase genes in *Drosophila*, totaling 214 target genes.

Larger mechanomic screens have previously been performed using different mechanical phenotyping methods. Toyoda et al. (22) conducted a RNAi-based screen of over 1,000 human genes using atomic force microscopy (AFM), including targets involved in the actomyosin cortex, membrane-associated transporters, and kinases, specifically analyzing the mechanical properties of mitotic cells. However, the low throughput of AFM limited their measurements to only a few cells per knockdown condition, compared RT-FDC's high-throughput capacity of thousands of cells per condition, increasing their screens susceptibility to sampling bias. Han et al. (43) employed a pooled CRISPR-Cas9-mediated loss-of-function screen targeting 507 human kinase genes using microfluidic sorting to identify gene knockouts overrepresented among softer mechanical phenotypes. While this approach significantly increased throughput compared to AFM, it lacked single-cell resolution, providing no detailed stiffness distributions for individual gene knockouts. Thus, RT-FDC uniquely combines high throughput with single-cell resolution, addressing the limitations of both methods.

By comparing our results to these previous studies via cross-species homology, we observed partial overlap in identified hits. Of the 71 kinases targeted in our study, 66 were also tested by Toyoda et al. (22), identifying 11 as mechanical hits; two of these hits (*hppy*, *hop*) were replicated in our study. Similarly, Han et al. (43) tested 54 kinases targeted in our screen, identifying seven hits, five of which overlapped with ours (*p38b*, *hop*, *sgg*, *aurA*, *slpr*). This cross-species validation underscores the conserved role of these kinase pathways in mechanical regulation.

Notably, the *Drosophila* JAK homolog *hop* (*hopscotch*), identified in all three screens, had never been directly linked to cell mechanics. However, evidence from human studies suggests that the JAK signaling pathway may play a role in mechanical regulation (44, 45). The identification of the *JAK* homolog *hop* in all three screens provides additional support for this hypothesis and highlights the potential of genome-scale screening methods such as RT-FDC to uncover novel gene functions related to cell mechanics.

CONCLUSION

We presented a genome-scale RNA interference (RNAi) knockdown screen investigating the roles of kinase and phosphatase genes in regulating single-cell mechanical phenotypes using Real-Time Fluorescence and Deformability Cytometry (RT-FDC). With 214 targeted genes, this study represents the largest deformability cytometry-based screen conducted to date. RT-FDC uniquely combines a high throughput of up to 100 cells/s with single-cell resolution, enabling comprehensive sampling of mechanical phenotype distributions within knockdown cell populations. Additionally, its capability to separately analyze interphase and mitotic cells allowed us to overcome the bias of population-wide analyses against softening and mitosis-specific knockdown effects, as well as identifying apparent stiffening effects caused by underlying shifts in cell cycle distribution.

By identifying both known and novel mechanical regulators across diverse cellular processes, our results establish RT-FDC as a robust and versatile platform for large-scale mechanomic screening. Furthermore, the newly discovered mechanical regulators uncovered in our study, such as *PRL-1* and *hop*, provide valuable starting points for future investigations into genotype-phenotype relationships. Moving forward, mechanistic follow-up studies on both known and newly identified regulators will be essential for further unraveling how signaling pathways orchestrate structural determinants of cell mechanical phenotypes in both physiological and disease contexts.

While our screen focused exclusively on cell stiffness quantified through a single Young's modulus value, it is well-established that cells are viscoelastic, exhibiting both solid-like elastic and fluid-like viscous properties (46–48). Thus, representing cell mechanics by a single elastic modulus measured at sub-second time scales, as performed by RT-FDC, may overlook important viscous contributions and time-dependent deformation characteristics relevant to physiological conditions (see (15) for a detailed discussion). Recent advances in deformability cytometry address this limitation by leveraging the inherent modularity of the technique, allowing measurement modes to be adapted by simply exchanging the microfluidic chip design and adjusting the post-experimental data analysis pipeline. Examples include high-throughput viscoelastic phenotyping using hyperbolic microchannels (49) or the Microfluidic Microcirculation Mimetic (MMM), which analyzes cell traversal through microvascular-like constrictions (50). The modularity of deformability cytometry facilitates straightforward adaptation of our screening approach to these advanced viscoelastic measurement techniques. We therefore anticipate future mechanomic screens incorporating viscoelastic phenotyping, enabling the identification of genetic regulators of cellular viscosity, and thus providing a more comprehensive understanding of cell mechanics beyond the current cytoskeleton-centered view.

AUTHOR CONTRIBUTIONS

J.G and B.B. designed the research and supervised the project. K.P., C.S and C.L. performed the experiments. L.S. and K.P. analyzed the data. P.M. maintained analysis and data management software. L.S. and J.K. wrote the article.

ACKNOWLEDGMENTS

We want to thank Martin Kräter, Benedikt Hartmann, Nico Appold und Maximilian Eiche for helpful discussion regarding this study. Additional thanks to Eoghan O'Connell for help with data analysis. The authors acknowledge the financial support through the core funding of the Max Planck Society to JG and the Emmy Noether Programme of the German Research Foundation (455449456) to JK. BB received funding from Cancer Research UK: CRUK Programme Grant (C1529/A17343) and CRUK/EPSRC Multi-Disciplinary Project Award (C1529/A23335).

DECLARATION OF GENERATIVE AI AND AI-ASSISTED TECHNOLOGIES IN THE WRITING PROCESS

During the preparation of this work the authors used ChatGPT-4o and o1 in order to improve readability and language. After using this tool, the authors reviewed and edited the content as needed and take full responsibility for the content of the publication.

DECLARATION OF INTERESTS

The authors declare no competing interests.

REFERENCES

1. Lange, J. R., and B. Fabry, 2013. Cell and tissue mechanics in cell migration. *Experimental Cell Research* 319:2418–2423. https://www.sciencedirect.com/science/article/pii/S0014482713001948.

2. Miller, A. E., P. Hu, and T. H. Barker, 2020. Feeling Things Out: Bidirectional Signaling of the Cell–ECM Interface, Implications in the Mechanobiology of Cell Spreading, Migration, Proliferation, and Differentiation. *Advanced Healthcare Materials* 9:1901445. https://onlinelibrary.wiley.com/doi/abs/10.1002/adhm.201901445, _eprint: https://onlinelibrary.wiley.com/doi/pdf/10.1002/adhm.201901445.

3. De Belly, H., E. K. Paluch, and K. J. Chalut, 2022. Interplay between mechanics and signalling in regulating cell fate. *Nature Reviews Molecular Cell Biology* 23:465–480. https://www.nature.com/articles/s41580-022-00472-z, publisher: Nature Publishing Group.

4. Bongiorno, T., J. Kazlow, R. Mezencev, S. Griffiths, R. Olivares-Navarrete, J. F. McDonald, Z. Schwartz, B. D. Boyan, T. C. McDevitt, and T. Sulchek, 2014. Mechanical stiffness as an improved single-cell indicator of osteoblastic human mesenchymal stem cell differentiation. *Journal of Biomechanics* 47:2197–2204. https://www.sciencedirect.com/science/article/pii/S0021929013005691.

5. Li, X., M. Dao, G. Lykotrafitis, and G. E. Karniadakis, 2017. Biomechanics and biorheology of red blood cells in sickle cell anemia. *Journal of Biomechanics* 50:34–41. https://www.sciencedirect.com/science/article/pii/S0021929016311903.

6. Toepfner, N., C. Herold, O. Otto, P. Rosendahl, A. Jacobi, M. Kräter, J. Stächele, L. Menschner, M. Herbig, L. Ciuffreda, L. Ranford-Cartwright, M. Grzybek, Ü. Coskun, E. Reithuber, G. Garriss, P. Mellroth, B. Henriques-Normark, N. Tregay, M. Suttorp, M. Bornhäuser, E. R. Chilvers, R. Berner, and J. Guck, 2018. Detection of human disease conditions by single-cell morpho-rheological phenotyping of blood. *eLife* 7:e29213. https://doi.org/10.7554/eLife.29213, publisher: eLife Sciences Publications, Ltd.

7. Kubánková, M., B. Hohberger, J. Hoffmanns, J. Fürst, M. Herrmann, J. Guck, and M. Kräter, 2021. Physical phenotype of blood cells is altered in COVID-19. *Biophysical Journal* 120:2838–2847. Publisher: Biophysical Society.

8. Renoux, C., R. Fort, E. Nader, C. Boisson, P. Joly, E. Stauffer, M. Robert, S. Girard, A. Cibiel, A. Gauthier, and P. Connes, 2021. Impact of COVID-19 on red blood cell rheology. *British Journal of Haematology* 192:e108–e111. https://onlinelibrary.wiley.com/doi/abs/10.1111/bjh.17306, _eprint: https://onlinelibrary.wiley.com/doi/pdf/10.1111/bjh.17306.

9. Dondorp, A. M., P. A. Kager, J. Vreeken, and N. J. White, 2000. Abnormal Blood Flow and Red Blood Cell Deformability in Severe Malaria. *Parasitology Today* 16:228–232. https://www.sciencedirect.com/science/article/pii/S0169475800016665.

10. Bashant, K. R., A. Vassallo, C. Herold, R. Berner, L. Menschner, J. Subburayalu, M. J. Kaplan, C. Summers, J. Guck, E. R. Chilvers, and N. Toepfner, 2019. Real-time deformability cytometry reveals sequential contraction and expansion during neutrophil priming. *Journal of Leukocyte Biology* 105:1143–1153. https://onlinelibrary.wiley.com/doi/abs/10.1002/JLB.MA0718-295RR, _eprint: https://onlinelibrary.wiley.com/doi/pdf/10.1002/JLB.MA0718-295RR.

11. Guck, J., S. Schinkinger, B. Lincoln, F. Wottawah, S. Ebert, M. Romeyke, D. Lenz, H. M. Erickson, R. Ananthakrishnan, D. Mitchell, J. Käs, S. Ulvick, and C. Bilby, 2005. Optical Deformability as an Inherent Cell Marker for Testing Malignant Transformation and Metastatic Competence. *Biophysical Journal* 88:3689–3698. https://www.cell.com/biophysj/abstract/S0006-3495(05)73417-2, publisher: Elsevier.

12. Lin, H.-H., H.-K. Lin, I.-H. Lin, Y.-W. Chiou, H.-W. Chen, C.-Y. Liu, H. I.-C. Harn, W.-T. Chiu, Y.-K. Wang, M.-R. Shen, and M.-J. Tang, 2015. Mechanical phenotype of cancer cells: cell softening and loss of stiffness sensing. *Oncotarget* 6:20946–20958. https://www.oncotarget.com/article/4173/text/, publisher: Impact Journals.

13. Roberts, A. B., J. Zhang, V. Raj Singh, M. Nikolić, E. Moeendarbary, R. D. Kamm, P. T. C. So, and G. Scarcelli, 2021. Tumor cell nuclei soften during transendothelial migration. *Journal of Biomechanics* 121:110400. https://www.sciencedirect.com/science/article/pii/S0021929021001809.

14. Alibert, C., B. Goud, and J.-B. Manneville, 2017. Are cancer cells really softer than normal cells? *Biology of the Cell* 109:167–189. https://onlinelibrary.wiley.com/doi/abs/10.1111/boc.201600078, _eprint: https://onlinelibrary.wiley.com/doi/pdf/10.1111/boc.201600078.

15. Urbanska, M., and J. Guck, 2024. Single-Cell Mechanics: Structural Determinants and Functional Relevance. *Annual Reviews* https://www.annualreviews.org/content/journals/10.1146/annurev-biophys-030822-030629, publisher: Annual Reviews.

16. Lei, K., A. Kurum, M. Kaynak, L. Bonati, Y. Han, V. Cencen, M. Gao, Y.-Q. Xie, Y. Guo, M. T. M. Hannebelle, Y. Wu, G. Zhou, M. Guo, G. E. Fantner, M. S. Sakar, and L. Tang, 2021. Cancer-cell stiffening via cholesterol depletion enhances adoptive T-cell immunotherapy. *Nature Biomedical Engineering* 5:1411–1425. https://www.nature.com/articles/s41551-021-00826-6, publisher: Nature Publishing Group.

17. Kelkar, M., P. Bohec, and G. Charras, 2020. Mechanics of the cellular actin cortex: From signalling to shape change. *Current Opinion in Cell Biology* 66:69–78. https://www.sciencedirect.com/science/article/pii/S0955067420300739.

18. Grady, M. E., R. J. Composto, and D. M. Eckmann, 2017. Cytoskeletal Perturbing Drugs and Their Effect on Cell Elasticity. *In* C. S. Korach, S. A. Tekalur, and P. Zavattieri, editors, Mechanics of Biological Systems and Materials, Volume 6. Springer International Publishing, Cham, 169–177.

19. Hargreaves, A. J., 1997. The Cytoskeleton as a Target in Cell Toxicity. *In* E. E. Bittar, editor, Advances in Molecular and Cell Biology, Elsevier, volume 20 of *Mechanisms of Cell Toxicity*, 119–144. https://www.sciencedirect.com/science/article/pii/S1569255808602738.

20. Wilson, R. C., and J. A. Doudna, 2013. Molecular Mechanisms of RNA Interference. *Annual Review of Biophysics* 42:217–239. https://www.annualreviews.org/content/journals/10.1146/annurev-biophys-083012-130404, publisher: Annual Reviews.

21. Chugh, P., A. G. Clark, M. B. Smith, D. A. D. Cassani, K. Dierkes, A. Ragab, P. P. Roux, G. Charras, G. Salbreux, and E. K. Paluch, 2017. Actin cortex architecture regulates cell surface tension. *Nature Cell Biology* 19:689–697. https://www.nature.com/articles/ncb3525, publisher: Nature Publishing Group.

22. Toyoda, Y., C. J. Cattin, M. P. Stewart, I. Poser, M. Theis, T. V. Kurzchalia, F. Buchholz, A. A. Hyman, and D. J. Müller, 2017. Genome-scale single-cell mechanical phenotyping reveals disease-related genes involved in mitotic rounding. *Nature Communications* 8:1266. https://www.nature.com/articles/s41467-017-01147-6, publisher: Nature Publishing Group.

23. Urbanska, M., Y. Ge, M. Winzi, S. Abuhattum, S. S. Ali, M. Herbig, M. Kräter, N. Toepfner, J. Durgan, O. Florey, M. Dori, F. Calegari, F.-N. Lolo, M. Á. d. Pozo, A. Taubenberger, C. V. Cannistraci, and J. Guck, 2023. De novo identification of universal cell mechanics gene signatures. *eLife* 12. https://elifesciences.org/reviewed-preprints/87930, publisher: eLife Sciences Publications Limited.

24. Su, T. T., 2019. Drug screening in Drosophila; why, when, and when not? *WIREs Developmental Biology* 8:e346. https://onlinelibrary.wiley.com/doi/abs/10.1002/wdev.346, _eprint: https://onlinelibrary.wiley.com/doi/pdf/10.1002/wdev.346.

25. Boutros, M., and J. Ahringer, 2008. The art and design of genetic screens: RNA interference. *Nature Reviews Genetics* 9:554–566. https://www.nature.com/articles/nrg2364, publisher: Nature Publishing Group.

26. Jacobi, A., P. Rosendahl, M. Kräter, M. Urbanska, M. Herbig, and J. Guck, 2019. Analysis of Biomechanical Properties of Hematopoietic Stem and Progenitor Cells Using Real-Time Fluorescence and Deformability Cytometry. *In* G. Klein, and P. Wuchter, editors, Stem Cell Mobilization: Methods and Protocols, Springer, New York, NY, Methods in Molecular Biology, 135–148. https://doi.org/10.1007/978-1-4939-9574-5_11.

27. Mokbel, M., D. Mokbel, A. Mietke, N. Träber, S. Girardo, O. Otto, J. Guck, and S. Aland, 2017. Numerical Simulation of Real-Time Deformability Cytometry To Extract Cell Mechanical Properties. *ACS Biomaterials Science & Engineering* 3:2962–2973. https://doi.org/10.1021/acsbiomaterials.6b00558, publisher: American Chemical Society.

28. Urbanska, M., H. E. Muñoz, J. Shaw Bagnall, O. Otto, S. R. Manalis, D. Di Carlo, and J. Guck, 2020. A comparison of microfluidic methods for high-throughput cell deformability measurements. *Nature Methods* 17:587–593. https://www.nature.com/articles/s41592-020-0818-8, number: 6 Publisher: Nature Publishing Group.

29. Rosendahl, P., K. Plak, A. Jacobi, M. Kraeter, N. Toepfner, O. Otto, C. Herold, M. Winzi, M. Herbig, Y. Ge, S. Girardo, K. Wagner, B. Baum, and J. Guck, 2018. Real-time fluorescence and deformability cytometry. *Nature Methods* 15:355–358. https://www.nature.com/articles/nmeth.4639, number: 5 Publisher: Nature Publishing Group.

30. Matei, A.-E., M. Kubánková, L. Xu, A.-H. Györfi, E. Boxberger, D. Soteriou, M. Papava, J. Prater, X. Hong, C. Bergmann, M. Kräter, G. Schett, J. Guck, and J. H. W. Distler, 2023. Identification of a Distinct Monocyte-Driven Signature in Systemic Sclerosis Using Biophysical Phenotyping of Circulating Immune Cells. *Arthritis & Rheumatology* 75:768–781. https://onlinelibrary.wiley.com/doi/abs/10.1002/art.42394, _eprint: https://onlinelibrary.wiley.com/doi/pdf/10.1002/art.42394.

31. Ostalé, C. M., N. Esteban, A. López-Varea, and J. F. de Celis, 2021. Functional requirements of protein kinases and phosphatases in the development of the Drosophila melanogaster wing. *G3 Genes|Genomes|Genetics* 11:jkab348. https://doi.org/10.1093/g3journal/jkab348.

32. Horn, T., T. Sandmann, and M. Boutros, 2010. Design and evaluation of genome-wide libraries for RNA interference screens. *Genome Biology* 11:R61. https://doi.org/10.1186/gb-2010-11-6-r61.

33. Herbig, M., M. Kräter, K. Plak, P. Müller, J. Guck, and O. Otto, 2018. Real-Time Deformability Cytometry: Label-Free Functional Characterization of Cells. *In* T. S. Hawley, and R. G. Hawley, editors, Flow Cytometry Protocols, Springer, New York, NY, Methods in Molecular Biology, 347–369. https://doi.org/10.1007/978-1-4939-7346-0_15.

34. Herbig, M., A. Mietke, P. Müller, and O. Otto, 2018. Statistics for real-time deformability cytometry: Clustering, dimensionality reduction, and significance testing. *Biomicrofluidics* 12:042214. https://doi.org/10.1063/1.5027197.

35. Thoma, O.-M., E. Naschberger, M. Kubánková, I. Larafa, V. Kramer, B. Menchicchi, S. Merkel, N. Britzen-Laurent, A. Jefremow, R. Grützmann, K. Koop, C. Neufert, R. Atreya, J. Guck, M. Stürzl, M. F. Neurath, and M. J. Waldner, 2024. p21 Prevents the Exhaustion of CD4+ T Cells Within the Antitumor Immune Response Against Colorectal Cancer. *Gastroenterology* 166:284–297.e11. https://www.sciencedirect.com/science/article/pii/S0016508523050084.

36. Reichel, F., M. Kräter, K. Peikert, H. Glaß, P. Rosendahl, M. Herbig, A. Rivera Prieto, A. Kihm, G. Bosman, L. Kaestner, A. Hermann, and J. Guck, 2022. Changes in Blood Cell Deformability in Chorea-Acanthocytosis and Effects of Treatment With Dasatinib or Lithium. *Frontiers in Physiology* 13. https://www.frontiersin.org/articles/10.3389/fphys.2022.852946.

37. Fujii, Y., W. C. Koizumi, T. Imai, M. Yokobori, T. Matsuo, K. Oka, K. Hotta, and T. Okajima, 2021. Spatiotemporal dynamics of single cell stiffness in the early developing ascidian chordate embryo. *Communications Biology* 4:1–12. https://www.nature.com/articles/s42003-021-01869-w, publisher: Nature Publishing Group.

38. Jang, J. K., A. C. Gladstein, A. Das, J. G. Shapiro, Z. L. Sisco, and K. S. McKim, 2021. Multiple pools of PP2A regulate spindle assembly, kinetochore attachments and cohesion in Drosophila oocytes. *Journal of Cell Science* 134:jcs254037. https://doi.org/10.1242/jcs.254037.

39. Helps, N. R., N. D. Brewis, K. Lineruth, T. Davis, K. Kaiser, and P. T. W. Cohen, 1998. Protein phosphatase 4 is an essential enzyme required for organisation of microtubules at centrosomes in Drosophila embryos. *Journal of Cell Science* 111:1331–1340. https://doi.org/10.1242/jcs.111.10.1331.

40. Pagarigan, K. T., B. W. Bunn, J. Goodchild, T. K. Rahe, J. F. Weis, and L. J. Saucedo, 2013. Drosophila PRL-1 Is a Growth Inhibitor That Counteracts the Function of the Src Oncogene. *PLOS ONE* 8:e61084. https://journals.plos.org/plosone/article?id=10.1371/journal.pone.0061084, publisher: Public Library of Science.

41. Hosseini, K., A. Taubenberger, C. Werner, and E. Fischer-Friedrich, 2020. EMT-Induced Cell-Mechanical Changes Enhance Mitotic Rounding Strength. *Advanced Science* 7:2001276. https://onlinelibrary.wiley.com/doi/abs/10.1002/advs.202001276, _eprint: https://onlinelibrary.wiley.com/doi/pdf/10.1002/advs.202001276.

42. Golfier, S., P. Rosendahl, A. Mietke, M. Herbig, J. Guck, and O. Otto, 2017. High-throughput cell mechanical phenotyping for label-free titration assays of cytoskeletal modifications. *Cytoskeleton* 74:283–296. https://onlinelibrary.wiley.com/doi/abs/10.1002/cm.21369, _eprint: https://onlinelibrary.wiley.com/doi/pdf/10.1002/cm.21369.

43. Han, X., Z. Liu, L. Zhao, F. Wang, Y. Yu, J. Yang, R. Chen, and L. Qin, 2016. Microfluidic Cell Deformability Assay for Rapid and Efficient Kinase Screening with the CRISPR-Cas9 System. *Angewandte Chemie International Edition* 55:8561–8565. https://onlinelibrary.wiley.com/doi/abs/10.1002/anie.201601984, _eprint: https://onlinelibrary.wiley.com/doi/pdf/10.1002/anie.201601984.

44. Grote, K., M. Luchtefeld, and B. Schieffer, 2005. JANUS under stress—Role of JAK/STAT signaling pathway in vascular diseases. *Vascular Pharmacology* 43:357–363. https://www.sciencedirect.com/science/article/pii/S1537189105001904.

45. Sanz-Moreno, V., C. Gaggioli, M. Yeo, J. Albrengues, F. Wallberg, A. Viros, S. Hooper, R. Mitter, C. C. Féral, M. Cook, J. Larkin, R. Marais, G. Meneguzzi, E. Sahai, and C. J. Marshall, 2011. ROCK and JAK1 Signaling Cooperate to Control Actomyosin Contractility in Tumor Cells and Stroma. *Cancer Cell* 20:229–245. https://www.cell.com/cancer-cell/abstract/S1535-6108(11)00230-3, publisher: Elsevier.

46. Corominas-Murtra, B., and N. I. Petridou, 2021. Viscoelastic Networks: Forming Cells and Tissues. *Frontiers in Physics* 9. https://www.frontiersin.org/journals/physics/articles/10.3389/fphy.2021.666916/full, publisher: Frontiers.

47. Gerum, R., E. Mirzahossein, M. Eroles, J. Elsterer, A. Mainka, A. Bauer, S. Sonntag, A. Winterl, J. Bartl, L. Fischer, S. Abuhattum, R. Goswami, S. Girardo, J. Guck, S. Schrüfer, N. Ströhlein, M. Nosratlo, H. Herrmann, D. Schultheis, F. Rico, S. J. Müller, S. Gekle, and B. Fabry, 2022. Viscoelastic properties of suspended cells measured with shear flow deformation cytometry. *eLife* 11:e78823. https://doi.org/10.7554/eLife.78823, publisher: eLife Sciences Publications, Ltd.

48. Nguyen, T. L., E. R. Polanco, A. N. Patananan, T. A. Zangle, and M. A. Teitell, 2020. Cell viscoelasticity is linked to fluctuations in cell biomass distributions. *Scientific Reports* 10:7403. https://www.nature.com/articles/s41598-020-64259-y, publisher: Nature Publishing Group.

49. Reichel, F., R. Goswami, S. Girardo, and J. Guck, 2024. High-throughput viscoelastic characterization of cells in hyperbolic microchannels. *Lab on a Chip* 24:2440–2453. https://pubs.rsc.org/en/content/articlelanding/2024/lc/d3lc01061a, publisher: Royal Society of Chemistry.

50. Asuquo, M. I., E. Effa, O. Gbotosho, A. Otu, N. Toepfner, S. Ameh, S.-P. Bhayankaram, N. Zetocha, C. Nwakama, W. Egbe, J. Guck, and A. Ekpenyong, 2022. Microfluidic Microcirculation Mimetic as a Tool for the Study of Rheological Characteristics of Red Blood Cells in Patients with Sickle Cell Anemia. *Applied Sciences* 12:4394. https://www.mdpi.com/2076-3417/12/9/4394, number: 9 Publisher: Multidisciplinary Digital Publishing Institute.

51. Viquez, N. M., C. R. Li, Y. P. Wairkar, and A. DiAntonio, 2006. The B' Protein Phosphatase 2A Regulatory Subunit well-rounded Regulates Synaptic Growth and Cytoskeletal Stability at the Drosophila Neuromuscular Junction. *Journal of Neuroscience* 26:9293–9303. https://www.jneurosci.org/content/26/36/9293, publisher: Society for Neuroscience Section: Articles.

52. Martín-Blanco, E., A. Gampel, J. Ring, K. Virdee, N. Kirov, A. M. Tolkovsky, and A. Martinez-Arias, 1998. puckered encodes a phosphatase that mediates a feedback loop regulating JNK activity during dorsal closure in Drosophila. *Genes & Development* 12:557–570. http://genesdev.cshlp.org/content/12/4/557, company: Cold Spring Harbor Laboratory Press Distributor: Cold Spring Harbor Laboratory Press Institution: Cold Spring Harbor Laboratory Press Label: Cold Spring Harbor Laboratory Press Publisher: Cold Spring Harbor Lab.

53. Fernandez, R., F. Takahashi, Z. Liu, R. Steward, D. Stein, and E. R. Stanley, 2000. The Drosophila Shark tyrosine kinase is required for embryonic dorsal closure. *Genes & Development* 14:604–614. https://www.ncbi.nlm.nih.gov/pmc/articles/PMC316420/.

54. Diaz-Garcia, S., S. Ahmed, and A. Baonza, 2016. Analysis of the Function of Apoptosis during Imaginal Wing Disc Regeneration in Drosophila melanogaster. *PLoS ONE* 11:1–20. https://search.ebscohost.com/login.aspx?direct=true&db=aph&AN=119766109&site=ehost-live&scope=site, publisher: Public Library of Science.

55. Chen, D.-Y., M.-Y. Li, S.-Y. Wu, Y.-L. Lin, S.-P. Tsai, P.-L. Lai, Y.-T. Lin, J.-C. Kuo, T.-C. Meng, and G.-C. Chen, 2012. The Bro1-domain-containing protein Myopic/HDPTP coordinates with Rab4 to regulate cell adhesion and migration. *Journal of Cell Science* 125:4841–4852. https://doi.org/10.1242/jcs.108597.

56. Schumacher, S., T. Gryzik, S. Tannebaum, and H.-A. J. Müller, 2004. The RhoGEF Pebble is required for cell shape changes during cell migration triggered by the Drosophila FGF receptor Heartless. *Development* 131:2631–2640. https://doi.org/10.1242/dev.01149.

57. Niwa, R., K. Nagata-Ohashi, M. Takeichi, K. Mizuno, and T. Uemura, 2002. Control of Actin Reorganization by Slingshot, a Family of Phosphatases that Dephosphorylate ADF/Cofilin. *Cell* 108:233–246. https://www.cell.com/cell/abstract/S0092-8674(01)00638-9, publisher: Elsevier.

58. Hu, L., W. Brichalli, N. Li, S. Chen, Y. Cheng, Q. Liu, Y. Xiong, and J. Yu, 2022. Myotubularin functions through actomyosin to interact with the Hippo pathway. *EMBO reports* 23:e55851. https://www.embopress.org/doi/full/10.15252/embr.202255851, publisher: John Wiley & Sons, Ltd.

59. Townsend, L. N., H. Clarke, D. Maddison, K. M. Jones, L. Amadio, A. Jefferson, U. Chughtai, D. M. Bis, S. Züchner, N. D. Allen, W. Van der Goes van Naters, O. M. Peters, and G. A. Smith, 2023. Cdk12 maintains the integrity of adult axons by suppressing actin remodeling. *Cell Death Discovery* 9:1–12. https://www.nature.com/articles/s41420-023-01642-4, publisher: Nature Publishing Group.

60. Huang, D., X. Li, L. Sun, P. Huang, H. Ying, H. Wang, J. Wu, and H. Song, 2016. Regulation of Hippo signalling by p38 signalling. *Journal of Molecular Cell Biology* 8:328–337. https://doi.org/10.1093/jmcb/mjw036.

61. Jean, S., S. Cox, E. J. Schmidt, F. L. Robinson, and A. Kiger, 2012. Sbf/MTMR13 coordinates PI(3)P and Rab21 regulation in endocytic control of cellular remodeling. *Molecular Biology of the Cell* 23:2723–2740. https://www.molbiolcell.org/doi/10.1091/mbc.e12-05-0375, publisher: American Society for Cell Biology (mboc).

62. Conder, R., H. Yu, B. Zahedi, and N. Harden, 2007. The serine/threonine kinase dPak is required for polarized assembly of F-actin bundles and apical–basal polarity in the *Drosophila* follicular epithelium. *Developmental Biology* 305:470–482. https://www.sciencedirect.com/science/article/pii/S0012160607001510.

63. Ruan, W., H. Long, D. H. Vuong, and Y. Rao, 2002. Bifocal Is a Downstream Target of the Ste20-like Serine/Threonine Kinase Misshapen in Regulating Photoreceptor Growth Cone Targeting in *Drosophila*. *Neuron* 36:831–842. https://www.sciencedirect.com/science/article/pii/S0896627302010279.

64. Jia, L., R. Wang, and D. D. Tang, 2012. Abl regulates smooth muscle cell proliferation by modulating actin dynamics and ERK1/2 activation. *American Journal of Physiology-Cell Physiology* 302:C1026–C1034. https://journals.physiology.org/doi/full/10.1152/ajpcell.00373.2011, publisher: American Physiological Society.

65. Zheng, Y., W. Wang, B. Liu, H. Deng, E. Uster, and D. Pan, 2015. Identification of Happyhour/MAP4K as Alternative Hpo/Mst-like Kinases in the Hippo Kinase Cascade. *Developmental Cell* 34:642–655. https://www.sciencedirect.com/science/article/pii/S1534580715005481.

66. Ojelade, S. A., T. Jia, A. R. Rodan, T. Chenyang, J. L. Kadrmas, A. Cattrell, B. Ruggeri, P. Charoen, H. Lemaitre, T. Banaschewski, C. Büchel, A. L. W. Bokde, F. Carvalho, P. J. Conrod, H. Flor, V. Frouin, J. Gallinat, H. Garavan, P. A. Gowland, A. Heinz, B. Ittermann, M. Lathrop, S. Lubbe, J.-L. Martinot, T. Paus, M. N. Smolka, R. Spanagel, P. F. O'Reilly, J. Laitinen, J. M. Veijola, J. Feng, S. Desrivières, M.-R. Jarvelin, The IMAGEN Consortium, G. Schumann, and A. Rothenfluh, 2015. Rsu1 regulates ethanol consumption in Drosophila and humans. *Proceedings of the National Academy of Sciences* 112:E4085–E4093. https://www.pnas.org/doi/10.1073/pnas.1417222112, publisher: Proceedings of the National Academy of Sciences.

67. Franco, B., L. Bogdanik, Y. Bobinnec, A. Debec, J. Bockaert, M.-L. Parmentier, and Y. Grau, 2004. Shaggy, the Homolog of Glycogen Synthase Kinase 3, Controls Neuromuscular Junction Growth in Drosophila. *Journal of Neuroscience* 24:6573–6577. https://www.jneurosci.org/content/24/29/6573, publisher: Society for Neuroscience Section: BRIEF COMMUNICATIONS.

68. Komlós, M., J. Szinyákovics, G. Falcsik, T. Sigmond, B. Jezsó, T. Vellai, and T. Kovács, 2023. The Small-Molecule Enhancers of Autophagy AUTEN-67 and -99 Delay Ageing in Drosophila Striated Muscle Cells. *International Journal of Molecular Sciences* 24:8100. https://www.mdpi.com/1422-0067/24/9/8100, number: 9 Publisher: Multidisciplinary Digital Publishing Institute.

69. Gajewski, K. M., J. Wang, and R. A. Schulz, 2006. Calcineurin function is required for myofilament formation and troponin I isoform transition in *Drosophila* indirect flight muscle. *Developmental Biology* 289:17–29. https://www.sciencedirect.com/science/article/pii/S0012160605006688.

70. Zhao, A., S. Varady, M. O'Kelley-Bangsberg, V. Deng, A. Platenkamp, P. Wijngaard, M. Bern, W. Gormley, E. Kushkowski, K. Thompson, L. Tibbetts, A. T. Conner, D. Noeckel, A. Teran, A. Ritz, and D. A. Applewhite, 2023. From network analysis to experimental validation: identification of regulators of non-muscle myosin II contractility using the folded-gastrulation signaling pathway. *BMC Molecular & Cell Biology* 24:1–21. https://search.ebscohost.com/login.aspx?direct=true&db=aph&AN=172916517&site=ehost-live&scope=site, publisher: BioMed Central.

71. Jiang, Y., K. L. Scott, S.-J. Kwak, R. Chen, and G. Mardon, 2011. Sds22/PP1 links epithelial integrity and tumor suppression via regulation of myosin II and JNK signaling. *Oncogene* 30:3248–3260. https://search.ebscohost.com/login.aspx?direct=true&db=aph&AN=62976696&site=ehost-live&scope=site, publisher: Springer Nature.

72. Kirchner, J., S. Gross, D. Bennett, and L. Alphey, 2007. Essential, Overlapping and Redundant Roles of the Drosophila Protein Phosphatase 1α and 1β Genes. *Genetics* 176:273–281. https://doi.org/10.1534/genetics.106.069914.

73. Moon, W., and F. Matsuzaki, 2013. Aurora A kinase negatively regulates Rho-kinase by phosphorylation *in vivo*. *Biochemical and Biophysical Research Communications* 435:610–615. https://www.sciencedirect.com/science/article/pii/S0006291X13008103.

74. Duque, J., and N. Gorfinkiel, 2016. Integration of actomyosin contractility with cell-cell adhesion during dorsal closure. *Development* 143:4676–4686. https://doi.org/10.1242/dev.136127.

75. Nakayama, J., G. Xiao, K. Noma, A. Malikzay, P. Bjerling, K. Ekwall, R. Kobayashi, and S. I. Grewal, 2003. Alp13, an MRG family protein, is a component of fission yeast Clr6 histone deacetylase required for genomic integrity. *The EMBO Journal* 22:2776–2787. https://www.embopress.org/doi/full/10.1093/emboj/cdg248, num Pages: 2787 Publisher: John Wiley & Sons, Ltd.

76. Chen, F., V. Archambault, A. Kar, P. Lio', P. P. D'Avino, R. Sinka, K. Lilley, E. D. Laue, P. Deak, L. Capalbo, and D. M. Glover, 2007. Multiple Protein Phosphatases Are Required for Mitosis in *Drosophila*. *Current Biology* 17:293–303. https://www.sciencedirect.com/science/article/pii/S0960982207009384.

77. Lobert, V. H., M. L. Skardal, L. Malerød, J. E. Simensen, H. A. Algra, A. N. Andersen, T. Fleischer, H. A. Enserink, K. Liestøl, J. K. Heath, T. E. Rusten, and H. A. Stenmark, 2022. PHLPP1 regulates CFTR activity and lumen expansion through AMPK. *Development* 149:dev200955. https://doi.org/10.1242/dev.200955.

78. Wang, J., C. E. Kirby, and R. Herbst, 2002. The Tyrosine Phosphatase PRL-1 Localizes to the Endoplasmic Reticulum and the Mitotic Spindle and Is Required for Normal Mitosis *. *Journal of Biological Chemistry* 277:46659–46668. https://www.jbc.org/article/S0021-9258(19)33283-1/abstract, publisher: Elsevier.

79. Großhans, J., and E. Wieschaus, 2000. A Genetic Link between Morphogenesis and Cell Division during Formation of the Ventral Furrow in *Drosophila*. *Cell* 101:523–531. https://www.sciencedirect.com/science/article/pii/S0092867400808624.

80. Takeo, S., M. Tsuda, S. Akahori, T. Matsuo, and T. Aigaki, 2006. The Calcineurin Regulator Sra Plays an Essential Role in Female Meiosis in *Drosophila*. *Current Biology* 16:1435–1440. https://www.sciencedirect.com/science/article/pii/S0960982206016770.

81. Courtot, C., C. Fankhauser, V. Simanis, and C. F. Lehner, 1992. The Drosophila cdc25 homolog twine is required for meiosis. *Development* 116:405–416. https://doi.org/10.1242/dev.116.2.405.

82. Verstreken, P., T.-W. Koh, K. L. Schulze, R. G. Zhai, P. R. Hiesinger, Y. Zhou, S. Q. Mehta, Y. Cao, J. Roos, and H. J. Bellen, 2003. Synaptojanin Is Recruited by Endophilin to Promote Synaptic Vesicle Uncoating. *Neuron* 40:733–748. https://www.cell.com/neuron/abstract/S0896-6273(03)00644-5, publisher: Elsevier.

83. Hatzihristidis, T., N. Desai, A. P. Hutchins, T.-C. Meng, M. L. Tremblay, and D. Miranda-Saavedra, 2015. A *Drosophila*-centric view of protein tyrosine phosphatases. *FEBS Letters* 589:951–966. https://www.sciencedirect.com/science/article/pii/S001457931500143X.

84. Sun, L., M.-C. Yu, L. Kong, Z.-H. Zhuang, J.-H. Hu, and B.-X. Ge, 2008. Molecular identification and functional characterization of a *Drosophila* dual-specificity phosphatase DMKP-4 which is involved in PGN-induced activation of the JNK pathway. *Cellular Signalling* 20:1329–1337. https://www.sciencedirect.com/science/article/pii/S0898656808000892.

85. LEE, W.-J., S.-H. KIM, Y.-S. KIM, S.-J. HAN, K.-S. PARK, J.-H. RYU, M.-W. HUR, and K.-Y. CHOI, 2000. Inhibition of mitogen-activated protein kinase by a Drosophila dual-specific phosphatase. *Biochemical Journal* 349:821–828. https://doi.org/10.1042/bj3490821.

86. Zeidler, M. P., E. A. Bach, and N. Perrimon, 2000. The roles of the Drosophila JAK/STAT pathway. *Oncogene* 19:2598–2606. https://www.nature.com/articles/1203482, publisher: Nature Publishing Group.

87. Poon, C. L. C., W. Liu, Y. Song, M. Gomez, Y. Kulaberoglu, X. Zhang, W. Xu, A. Veraksa, A. Hergovich, A. Ghabrial, and K. F. Harvey, 2018. A Hippo-like Signaling Pathway Controls Tracheal Morphogenesis in Drosophila melanogaster. *Developmental Cell* 47:564–575.e5. https://www.cell.com/developmental-cell/abstract/S1534-5807(18)30821-9, publisher: Elsevier.

88. Mirkovic, I., K. Charish, S. M. Gorski, K. McKnight, and E. M. Verheyen, 2002. Drosophila *nemo* is an essential gene involved in the regulation of programmed cell death. *Mechanisms of Development* 119:9–20. https://www.sciencedirect.com/science/article/pii/S0925477302002897.

89. Baril, C., M. Sahmi, D. Ashton-Beaucage, B. Stronach, and M. Therrien, 2009. The PP2C Alphabet Is a Negative Regulator of Stress-Activated Protein Kinase Signaling in Drosophila. *Genetics* 181:567–579. https://doi.org/10.1534/genetics.108.096461.

90. Pojer, J. M., S. A. Manning, B. Kroeger, S. Kondo, and K. F. Harvey, 2021. The Hippo pathway uses different machinery to control cell fate and organ size. *iScience* 24:102830. https://www.sciencedirect.com/science/article/pii/S2589004221007987.

91. Benbahouche, N. E. H., I. Iliopoulos, I. Török, J. Marhold, J. Henri, A. V. Kajava, R. Farkaš, T. Kempf, M. Schnölzer, P. Meyer, I. Kiss, E. Bertrand, B. M. Mechler, and B. Pradet-Balade, 2014. *Drosophila* Spag Is the Homolog of RNA Polymerase II-associated Protein 3 (RPAP3) and Recruits the Heat Shock Proteins 70 and 90 (Hsp70 and Hsp90) during the Assembly of Cellular Machineries. *Journal of Biological Chemistry* 289:6236–6247. https://www.sciencedirect.com/science/article/pii/S0021925820440827.

92. Papakyrikos, A. M., M. J. Kim, and X. Wang, 2020. *Drosophila* PTPMT1 Has a Function in Tracheal Air Filling. *iScience* 23:101285. https://www.sciencedirect.com/science/article/pii/S2589004220304727.

TABLES

Table 1: Classification of gene function for known regulators of cell mechanics identified by the mechanomic screen according to literature. Genes only implicated in mitotic mechanics are instead classified as mitotic regulators. I/M for interphase- or mitosis-specific gene knockdown effects. P/K for phosphatase or kinase gene.

Gene	Cell Cycle	Enzyme Type	Cellular Function	Source
mts	I	P	actomyosin cortex	(51)
Pp2A-29B	M	P	actomyosin cortex	(51)
puc	I	P	actomyosin cortex	(52)
Shark	I	K	actomyosin cortex	(53)
slpr	M	K	actomyosin cortex	(54)
mop	I	P	cell migration and adhesion	(55)
htl	I	K	cell migration and adhesion	(56)
ssh	I	P	F-actin	(57)
mtm	I	P	F-actin	(58)
Cdk12	I	K	F-actin	(59)
p38b	I	K	F-actin	(60)
Pi3K68D	I	K	F-actin	(61)
Lar	M	P	F-actin	(62)
bif	M	P	F-actin	(63)
Abl	-[a]	K	F-actin	(64)
hppy	I	K	mechanotransduction	(65)
ics	I	K	mechanotransduction	(66)
sgg	I	K	microtubule	(67)
EDTP	I	P	muscle contractility	(68)
CanB2	I	P	muscle contractility	(69)
flw	I, M	P	myosin II	(70)
sds22	I, M	P	myosin II	(71)
Pp1α-96A	I	P	myosin II	(72)
aurA	I, M	K	myosin II	(73)
Mbs	M	P	myosin II	(74)

[a] *Abl* knockdown caused a significant mechanical shift in the full population, but not in either cell cycle subpopulation. As this shift could not be attributed to an increase in mitotic fraction, it is considered a genuine mechanical hit.

SUPPLEMENTARY MATERIAL

Supplemental Table S1: List of all targeted genes, their dsRNA strands used for RNAi knockdown and their sample IDs used during measurement and analysis of the screen.

Supplemental Table S2: List of all mechanical hits identfied in any of these four analyses groups: Full population, interphase, mitosis, full population reanalysis after mitotic downsampling. For each gene, its mitotic fraction change upon knockdown and its Young's modulus change, significance and error margins for each analysis identifying it as a mechanical hit are recorded.

Table 2: Known regulators of mitosis or meiosis identified by the mechanomic screen according to literature. I/M for interphase- or mitosis-specific gene knockdown effects. P/K for phosphatase or kinase gene.

Gene	Cell Cycle	Enzyme Type	Source
Alp13	M	P	(75)
aurB	I	K	(38)
csw	I	P	(76)
Mtmr6	I	P	(76)
Phlpp	I	P	(77)
Pp4-19C	M	P	(76)
PpD3	M	P	(76)
PPP4R2r	I	P	(76)
PRL-1	I, M	P	(78)
Ptp61F	I	P	(76)
PTP-ER	I	P	(76)
stg	I, M	P	(76)
trbl	M	K	(79)
tws	I, M	P	(76)
wdb	M	P	(38)
Pp2B-14D	M	P	(80)
twe	I	P	(81)

Table 3: Classification of gene function for genes neither implicated in mechanical nor mitotic regulation identified by the cell cycle-resolved mechanomic screen according to literature. I/M for interphase- or mitosis-specific gene knockdown effects. P/K for phosphatase or kinase gene. Genes whose function is not well established beyond their general kinase or phosphatase function are not listed.

Gene	Cell Cycle	Enzyme Type	Cellular Function	Source
Synj	I	P	neural function	(82)
Ptp10D	I	P	neural function	(83)
Ptp4E	I	P	neural function	(83)
MKP-4	I,M	P	signal transduction	(84)
Mkp	I,M	P	signal transduction	(85)
hop	I	K	signal transduction	(86)
GckIII	I	K	signal transduction	(87)
nmo	I	K	signal transduction	(88)
alph	I	P	signal transduction	(89)
Pez	I	P	signal transduction	(90)
spag	M	P	cellular machineries	(91)
PTPMT1	I,M	P	cellular machineries	(92)